

## CRACK SPACING IN REINFORCED ELEMENTS

L.J. Sluys and M.A. Brioschi<sup>1</sup>

Delft University of Technology, Department of Civil Engineering,  
Delft, The Netherlands.

### Abstract

The proper prediction of the width and the spacing of primary cracks in reinforced elements is subject of this paper. Attention is focused on the influence of the crack concept. A comparison has been made between standard crack models and the gradient crack model. The effect of the inclusion of a length scale parameter on the crack spacing is determined. Furthermore, attention is paid to the crucial role of the bond-slip characteristic in predicting crack spacing in reinforced elements.

### 1 Introduction

A number of computational issues related to the modelling of failure in reinforced elements will be addressed. In the paper we focus on the proper prediction of the width and the spacing of primary cracks in reinforced concrete. A level of modelling is adopted in which the traction-slip behaviour is explicitly taken into account via interface elements. In this fashion the influence of the material characteristics for concrete, bond-slip and steel on the crack spacing can be analysed.

If we use a standard crack model for the description of the concrete a mesh sensitivity occurs during the formation of a pattern of primary cracks. The width of a single primary crack and the spacing between the primary cracks is affected by the discretisation, i.e. a smaller element size results in a smaller crack width and in a smaller distance

---

1. On leave from the Politecnico di Milano, Dipartimento di Ingegneria Strutturale

between the cracks. On the other hand, when a pattern of cracks has developed fully the behaviour is mainly determined by the steel and no additional spurious mesh size effects occur. It will be shown that enhancing the model by including the fracture energy as a separate material parameter does not solve the problem. Namely, for reinforced concrete the amount of energy that is released by a fully developed pattern of primary cracks is determined by, firstly, the energy consumption of a single crack and, secondly, the crack spacing. It will be shown that this latter quantity is not predicted correctly with a so-called fracture energy-type model.

To remedy this improper behaviour the standard continuum model must be enriched by adding higher-order terms, either spatially or in the time domain. These models introduce a length scale parameter that reflects the inhomogeneous micro-structure of the material. This parameter sets the size of the fracture process zone. In reinforced structures the introduction of this length scale through higher-order strain-gradient terms determines the failure mode and is proportional to the spacing of the primary cracks. Use of the gradient model removes the mesh dependence in the primary crack spacing and a comparison with experimentally measured values for the crack spacing may provide a physically realistic estimation of the length scale parameter. It will be shown that modelling of the bond-slip behaviour is of crucial importance.

The computational analyses have been carried out with a bar with one reinforcement bar loaded at both sides by a dynamic force. The dynamic case is easier to perform computationally. The evolution of the primary crack pattern follows the stress wave and, dependent on the crack formulation, primary cracks occur at more or less regular distances. In statics, on the other hand, the first primary cracks occur at imperfect locations and other cracks form in between which gives a value for the crack spacing. So, in dynamic computations no imperfections have to be included because the non-uniform solution is driven by the stress wave. The evolution of primary cracks is different from the static case but the resulting value for the crack spacing, except from a negligible rate effect, is of the same order.

## **2 Geometrical modelling of reinforced concrete**

A number of approaches for the finite element modelling of reinforced concrete can be distinguished. If the micro-behaviour in the vicinity of the reinforcing bar is of particular interest a modelling of the reinforcing bar with ribs that provide the mechanical interlock is required. By using such a computational model next to the primary or dominant cracks, secondary transverse cracks, longitudinal cracks and crushing in compressive zones close to the ribs can be analysed (Rots 1988). This approach is essential for a better understanding of the bond-slip behaviour between the concrete and the steel. For analyses of reinforced concrete members, however, the above approach that includes all possible mechanisms is too complicated. Dependent on the distribution of the reinforcement two approaches can be used. When the reinforcement is concentrated in a few dominant reinforcing bars the traction-slip behaviour can be lumped into interfaces. The width and spacing of the primary cracks can be studied with this type of modelling. On the other hand, when the concrete is densely reinforced not every reinforcing bar can be modelled separately and an embedded formulation is used to model the primary cracks. Tension-stiffening then accounts for the bond characteristics, but a true slip be-

behaviour between the concrete and the steel cannot be modelled. In the analyses it will be demonstrated that this slip behaviour dominates the spacing of the primary cracks.

In this paper we focus on the proper prediction of the width and the spacing of primary cracks in reinforced concrete. A level of modelling is adopted in which the traction-slip behaviour is explicitly taken into account via interface elements. In this fashion the influence of the material characteristics for concrete, bond-slip and steel on the crack spacing can be analysed. An example of the finite element idealisation of the composite material is shown in Figure 1, in which the steel reinforcement bars have been modelled with three-noded truss elements, and in which six-noded interface elements have been introduced for the modelling of bond-slip behaviour between the concrete and the reinforcement. The width  $i$  of the interface element (see Figure 1) is equal to zero, while the thickness of the interface element is equal to the periphery of the reinforcement bar. It is noted that such a model gives a small overestimation of the cross-sectional area because the reinforcement is modelled in addition to the beam. For this reason density and stiffness of the beam are slightly larger.

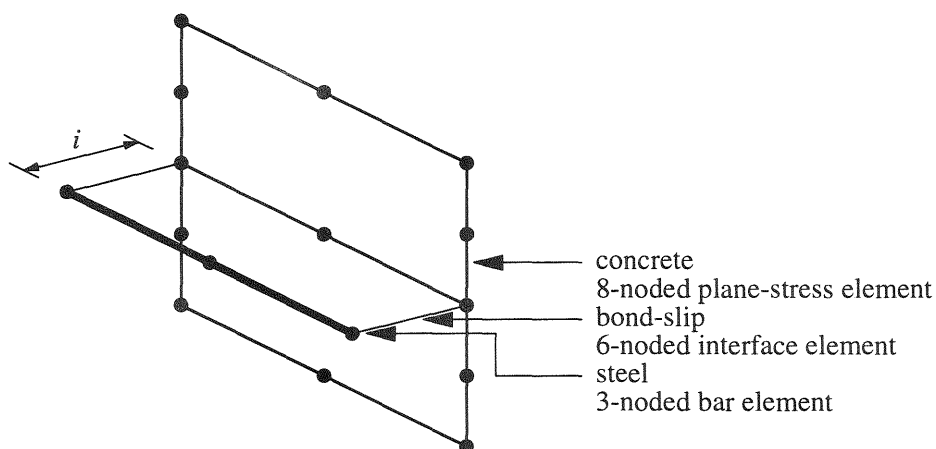


Fig. 1. Finite element idealisation of reinforced element.

### 3 Material modelling of reinforced concrete

The composite material consists of concrete and steel bars for which the distinct constitutive relations and interactive forces will be discussed in this section. The interactive forces between the concrete and the steel bars are determined via a bond-slip relation, which is the constitutive equation of the interface elements. For the concrete we use a smeared model in which the crack is conceived to be a continuum which permits a description in terms of stress-strain relations. We use three different concepts, namely the standard crack concept, the  $G_f$ -type crack concept and the strain-gradient dependent crack concept.

#### *Concrete : the standard crack model*

In the standard formulation for cracking we use a decomposition of total strain  $\varepsilon$  into an

elastic strain  $\varepsilon_e$  and a crack strain  $\varepsilon_{cr}$ . In a major principal stress direction a stress degradation takes place according to

$$\sigma = f_t + h\varepsilon_{cr} , \quad (1)$$

where  $\sigma$  denotes stress,  $f_t$  is the initial tensile strength and  $h$  is a constant negative softening modulus. The use of a standard model for cracking results in an ill-posed problem, i.e. under dynamic loading conditions each wave has an imaginary wave speed. As a consequence, a continuum discretised in finite elements always shows a crack zone which is only one element wide (*mesh sensitivity problem*). It appears that this solution for the cracked zone belongs to a wave with a speed equal to zero (stationary wave) and a width (wave length) equal to the finite element size (for linear elements see Sluys et.al.(1995)). In the standard continuum a length scale which sets the width of the fracture process zone and gives information on the non-homogeneous micro-structure of the concrete is lacking. In the discretised standard continuum this length scale is set by the size of the finite elements which makes the finite element simulation unreliable. This is also true for reinforced concrete in which the spacing between the primary cracks is affected by the mesh size as well. A smaller mesh size implies a faster degradation of stress and consequently a second primary crack will occur sooner and at a shorter distance of the first crack.

#### *Concrete : the $G_f$ -type crack model*

As an intermediate solution between using the standard continuum model and adding higher-order terms a number of authors (Pietruszczak and Mroz 1981, Bažant and Oh 1983, Willam 1984) have proposed to regard the area under the softening curve as a material parameter, namely the fracture energy  $G_f$

$$G_f = \int \sigma \varepsilon_{cr}(s) ds . \quad (2)$$

The fracture energy must be released over an equivalent length which for a standard model should correspond to a representative dimension of the mesh size. By doing this the slope of the strain-softening diagram has become a function of the finite element size. When we prescribe the fracture energy  $G_f$  as an additional material parameter the global load-displacement response can become insensitive to the discretisation. However, locally nothing has altered and localisation still takes place in one row of elements. This is logical, since the change of character of the partial differential equations occurs locally, even though the energy that is dissipated remains constant by adapting the softening modulus to the element size. For numerical simulations this implies for instance that severe convergence problems are usually encountered if the mesh is refined. Also, the frequently reported observation still holds that the localisation zones are biased by the discretisation and tend to propagate along the mesh lines. For reinforced elements the energy released in a single primary crack can be made mesh objective but the spacing between the primary cracks still depends on the finite element configuration.

#### *Concrete : the gradient crack model*

A model that can be used for the concrete to regularise the ill-posed problem is the strain-gradient dependent crack model (Aifantis 1984, Lasry and Belytschko 1988, Mühlhaus and Aifantis 1991, de Borst and Mühlhaus 1992, Sluys 1992, Pamin 1994). Higher-order strain gradients are introduced which represent nonlocal interactions at a

micro-structural level of the concrete. The model is formulated within a Rankine plasticity framework. An expression in one spatial direction reads

$$\sigma = f_t + h\varepsilon_{cr} + \bar{c} \frac{\partial^2 \varepsilon_{cr}}{\partial x^2}, \quad (3)$$

with  $\bar{c}$  a gradient parameter which can be regarded as a measure for the interaction length of micro-structural defects. A strain-gradient dependent continuum can only transmit waves with wave lengths smaller than a critical value. This critical value of the wave length belongs to a stationary wave (wave speed equal to zero) the wave length of which is determined by the length scale parameter in the model ( $l = \sqrt{\bar{c}/h}$ ). The stationary wave with the maximum wave length that is transmitted by the strain-gradient dependent continuum is the solution for the process zone of one primary crack (see Sluys et.al.(1995)). Mesh sensitivity is removed and the length scale parameter introduced in the model is a measure for the crack spacing as will be demonstrated in section 4.

#### *Steel reinforcement*

For the steel bars a simple elastic perfectly plastic relation has been used. In the analysis described in section 4 the response of the steel bars remains elastic.

#### *Bond-slip*

Experimental data for a normal bond component are hardly available and cannot be transformed into a constitutive law (Rots 1988). Therefore, the interface normal behaviour and the shear normal coupling are not incorporated and the constitutive equation for the interface element reduces to a shear traction - slip ( $\tau - \delta$ ) relation. This slip behaviour between reinforcement and concrete has been modelled using the relation of Dörr (Dörr 1980):

$$\tau = c [5.0(\delta/\delta_0) - 4.5(\delta/\delta_0)^2 + 1.4(\delta/\delta_0)^3] \quad \text{if } 0 < \delta < \delta_0 \quad (4)$$

$$\tau = 1.9c \quad \text{if } \delta > \delta_0, \quad (5)$$

in which  $c$  is a constant which is taken equal to the tensile strength  $f_t$  and  $\delta_0$  is the deformation at which perfect slip occurs which is usually taken equal to 0.06 mm.

## **4 Reinforcing bar**

The reinforcing bar is loaded at two sides by impact loads  $F(t)$ . The loading is such that cracking is initiated when the two loading waves meet in the centre of the bar while the response of the steel bar remains elastic. A relatively long bar is used to prevent that waves reflect at the two ends of the bar before the primary crack pattern has developed. The data set for the reinforcing bar problem is as follows (symbols are explained in Figure 2). The bar geometry is : length  $L = 4000$  mm, cross-section  $A = 100 \times 100$  mm<sup>2</sup> and a  $\varnothing 20$  reinforcement bar. The applied loading is distributed over the cross-section such that the interactive forces at both ends are zero, i.e  $F_0 = 18.3$  kN (15.0 kN on concrete and 3.3 kN on steel bar) and  $t_d = 0.00005$  s. For the concrete we have the Young's modulus  $E_c = 30000$  N/mm<sup>2</sup>, Poisson's ratio  $\nu = 0.2$ , density  $\rho = 2400$  kg/m<sup>3</sup>,  $f_t = 2.0$  N/mm<sup>2</sup> and  $\varepsilon_u = 0.001$ . For the  $G_f$ -type crack model the additional parameter is the finite element size, while for the gradient crack model the gradient constant  $\bar{c}$ , and implicitly the length scale  $l$ , is chosen. The algorithmic aspects of the mixed finite element

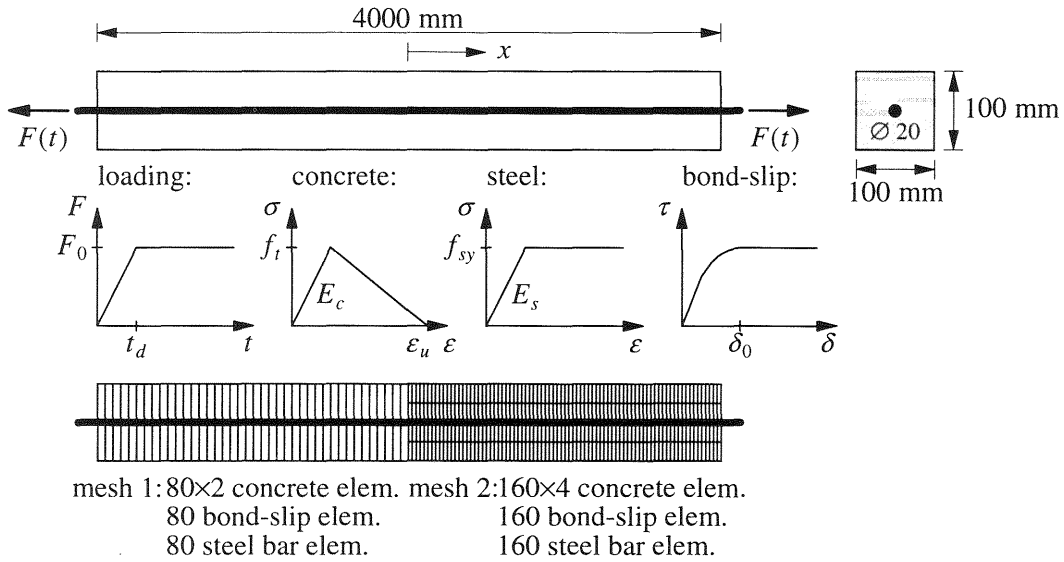


Fig. 2. Reinforcing bar

formulation for the gradient model with reduced integration are given in (Pamin 1994). The constitutive equation for the reinforcement reads :  $E_s = 210000 \text{ N/mm}^2$ ,  $\rho = 7800 \text{ kg/m}^3$  and  $f_{sy} = 500 \text{ N/mm}^2$  and for the bond-slip characteristic :  $c = 2.0 \text{ N/mm}^2$  and  $\delta_0 = 0.06 \text{ mm}$  (cf. eqn.(4)-(5)). The semi-discrete equations of motion have been solved with a Newmark time integration scheme with the updates

$$\dot{\mathbf{a}}^{t+\Delta t} = \dot{\mathbf{a}}^t + [(1-\gamma)\ddot{\mathbf{a}}^t + \gamma\ddot{\mathbf{a}}^{t+\Delta t}] \Delta t \quad (6)$$

and

$$\mathbf{a}^{t+\Delta t} = \mathbf{a}^t + \dot{\mathbf{a}}^t \Delta t + [(1/2-\beta)\ddot{\mathbf{a}}^t + \beta\ddot{\mathbf{a}}^{t+\Delta t}] \Delta t^2 \quad (7)$$

in which  $\ddot{\mathbf{a}}$ ,  $\dot{\mathbf{a}}$  and  $\mathbf{a}$  are the nodal accelerations, velocities and displacements, respectively. The integration constants are taken equal to  $\beta = 1/4$  and  $\gamma = 1/2$  corresponding to an average acceleration scheme. The time step in all analyses  $\Delta t = 2.5 \cdot 10^{-6} \text{ s}$  and a consistent mass matrix has been used. The Newmark scheme is used in combination with a full Newton-Raphson procedure to solve the nonlinear algebraic set of equations.

#### 4.1 Perfect bond

Perfect bond can be established by omitting the interface elements from the finite element geometry in Figure 1. If the response of the steel remains elastic perfect redistribution of stresses in the bar is obtained. The crack concept has been studied for the perfect bond case and the results are shown in the Figures 3, 4 and 5. In Figure 3 the strains in the concrete are given for the standard crack model with mesh 1 and mesh 2. The classical mesh-sensitivity problem for the crack width also plays a role for reinforced softening materials, namely all deformation per primary crack occurs in one vertical row

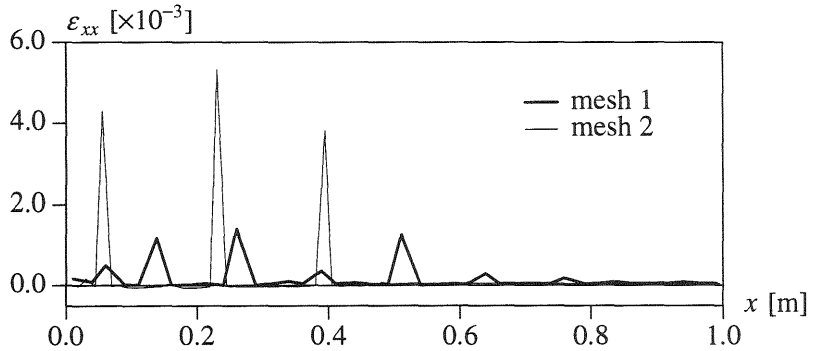


Fig. 3. Standard crack model - Perfect bond - mesh 1 and 2 -  $t = 0.0015$  s. Arbitrary locations of primary cracks.

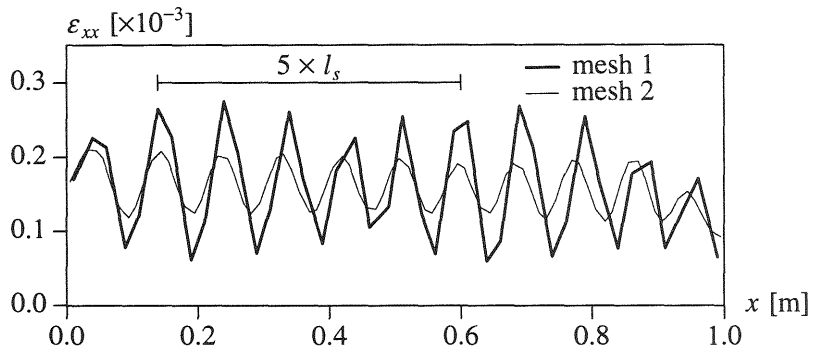


Fig. 4. Gradient crack model with  $l = 10$  mm - Perfect bond - mesh 1 and 2. Crack spacing  $l_s$  at  $t = 0.0015$  s.

of finite elements. For mesh 1 a number of cracks occur which decreases considerably by using mesh 2. So, the bar discretised with a finer mesh behaves more brittle (less energy per primary crack is consumed) which reduces the number of cracks. As will be discussed for the bond-slip case the results do not only depend on the finite element size but also on the time step, the time integration procedure and the mass discretisation (lumped, consistent). By not correctly predicting the crack spacing the amount of energy that is consumed in the bar is arbitrary and the results are unreliable. A  $G_f$ -type model does not improve the results. Although the amount of energy consumed per crack is more or less the same for mesh 1 and mesh 2, the location of the primary cracks and the crack spacing (related to the number of cracks) is arbitrary.

For the gradient model the results are different. Taking the length scale parameter  $l = 10$  mm gives a dense pattern of primary cracks (see Figure 4). The results no longer are arbitrary, i.e. for the two different meshes we obtain similar results, although mesh 1 is still a little bit too coarse to reproduce this crack pattern. For this case without the incorporation of bond-slip the length scale parameter can be related to the observed crack

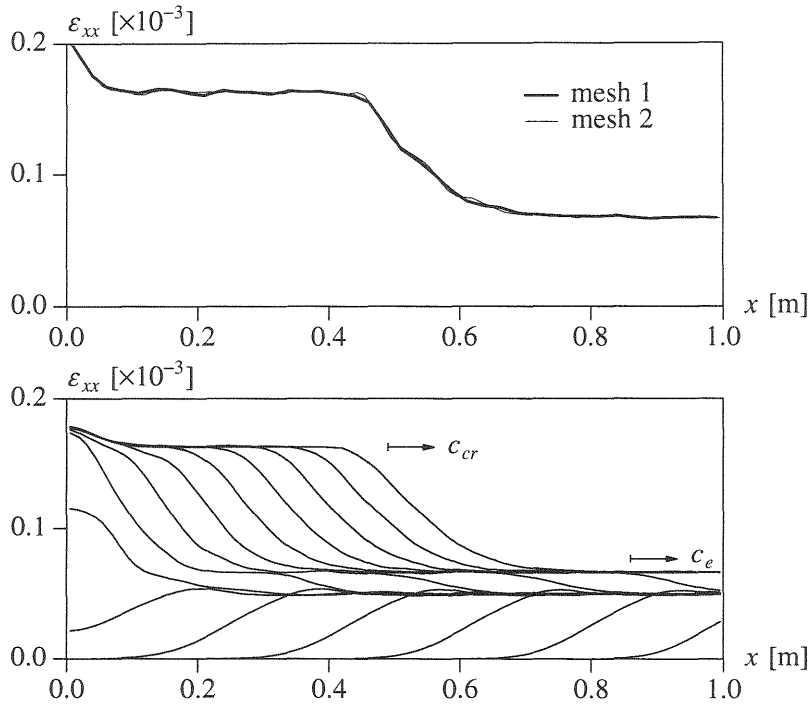


Fig. 5. Gradient crack model with  $l = 20$  mm - Perfect bond.  
 Top: Uniform distribution of strain in concrete at  $t = 0.001$  s.  
 Bottom: Stroboscopic evolution of strain in reinforcement  
 ( $0 < t < 0.001$  s).

spacing  $l_s$ . In this fashion the gradient constant  $\bar{c}$  can be determined on the basis of crack spacing measured in experiments. For an analysis with a length scale  $l = 20$  mm the results are given in Figure 5. For this analysis perfect redistribution of stress through the perfect bond behaviour shows a uniform distribution of crack strains over the bar. After the time that the two waves meet in the centre of the bar the elastic wave is split up into an elastic part ( $f_i - F_0/A$ ) which approximately propagates with the bar velocity  $c_e = \sqrt{E/\rho}$  and an inelastic part that causes cracking which propagates with speed  $c_{cr}$ . As shown in Figure 5 the strains in the reinforcement, which remain elastic, are the same as the total strains (sum of elastic and crack strain) in the concrete.

To consume the correct amount of strain energy for the case of perfect bond the area under the softening curve should not be  $G_f/e$ , with  $e$  the finite element size, as in the  $G_f$ -type crack model because then you will see an unlimited grow of consumed energy upon refinement of the mesh. This problem is opposite to the classical mesh-dependence problem for plain softening materials in which mesh refinement leads to a reduction of the strain energy. In conclusion, using the gradient crack model for the perfect bond case results not only in mesh-independent analyses but also in physically realistic analyses when the length scale is coupled to the crack spacing observed in experiments.



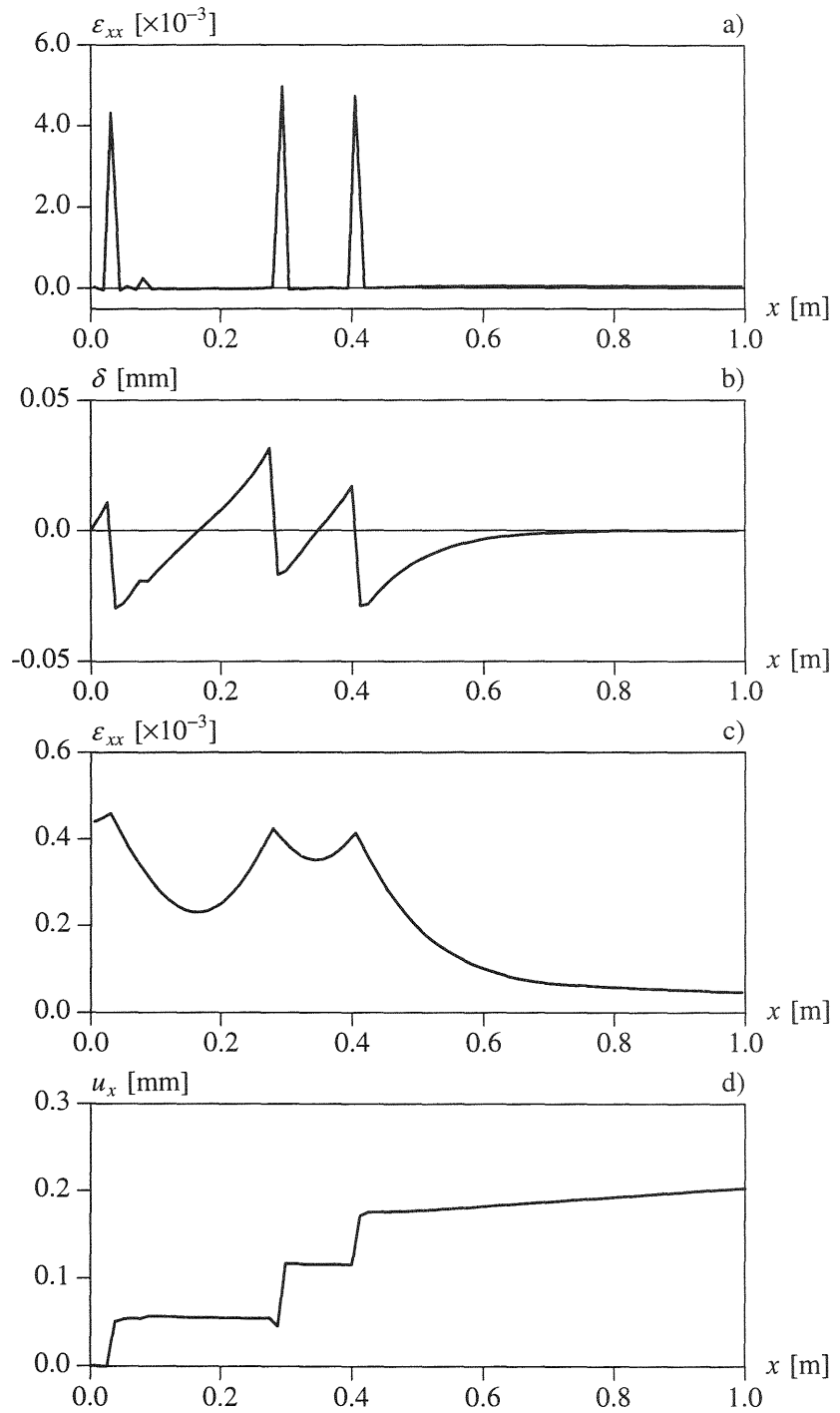


Fig. 6. Standard crack model - Bond-slip - mesh 2 -  $t = 0.0015$  s.  
a) Strain in concrete, b) shear deformation in interface,  
c) strain in steel and d) axial displacements.

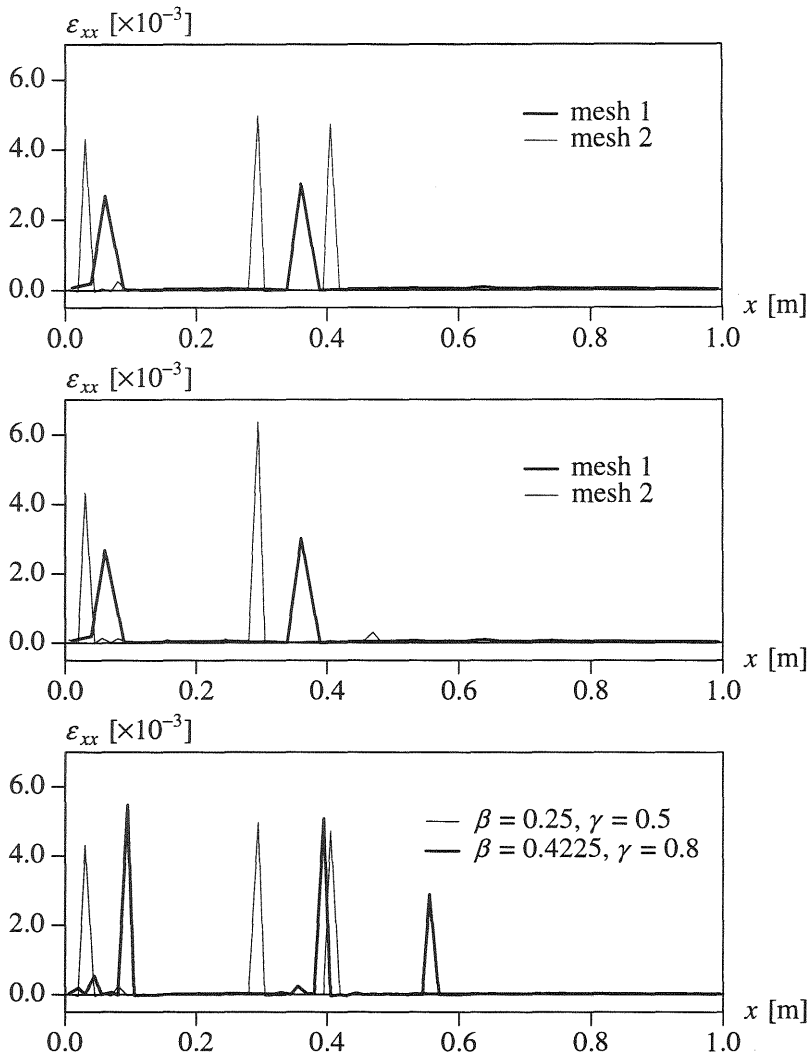


Fig. 7. Comparison of crack models - Bond-slip -  $t = 0.0015$  s.  
 Top: Standard crack model - mesh 1 and mesh 2.  
 Centre:  $G_f$ -type crack model - mesh 1 and mesh 2.  
 Bottom: Variation of time integration scheme - mesh 2.

## 4.2 Bond-slip

For the proper calculation of the crack spacing and the crack width the inclusion of bond-slip is crucial. To demonstrate the character of the solution for an analysis with the standard crack model Figure 6 shows the plots for the strains in the concrete and the steel, the shear deformation in the interface and the axial displacements. After the time the two waves meet a first primary crack appears. When the stress wave propagates further a second and a third primary crack occur. At the locations of primary cracks a steep gradient in slip in the interface element takes place. Although the response of the

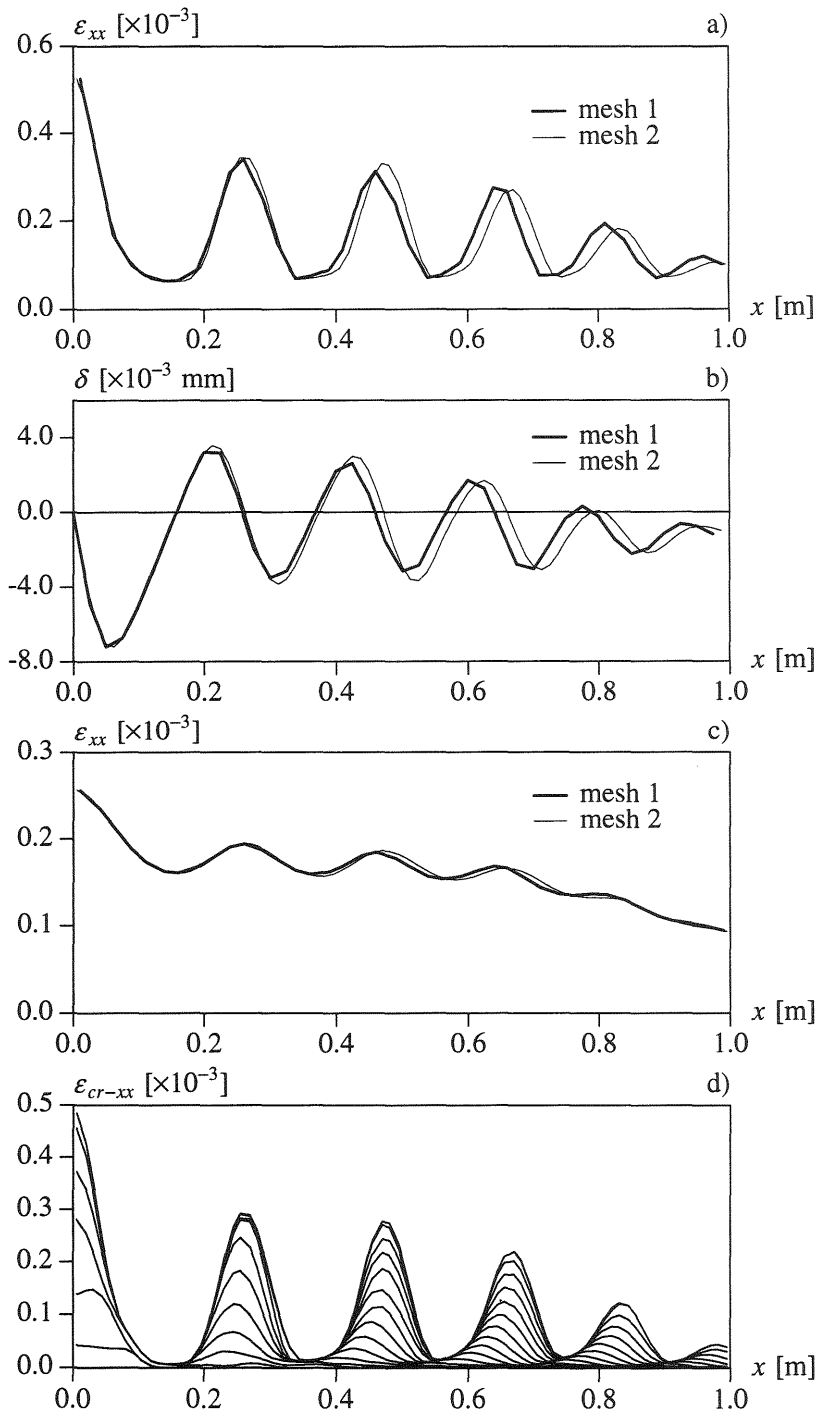


Fig. 8. Gradient crack model with  $l = 20$  mm - Bond-slip -  $t = 0.0015$  s.  
a) Strain in concrete, b) shear deformation in interface,  
c) strain in steel and d) stroboscopic development of crack strains.

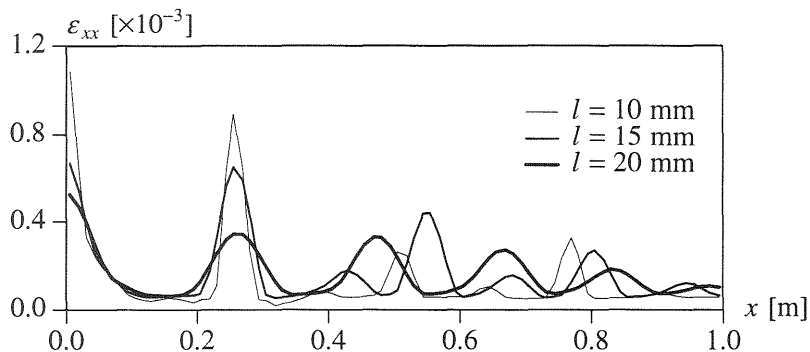


Fig. 9. Gradient crack model - Mesh 2 -  $t = 0.0015$  s.  
Variation of the length scale parameter.

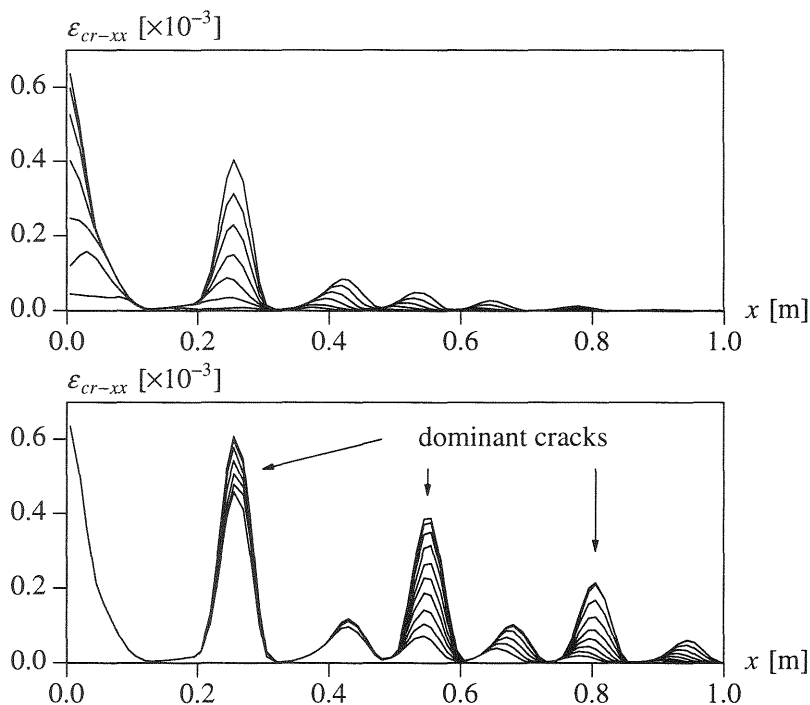


Fig. 10. Gradient crack model - Mesh 2 - Shift in primary crack pattern.  
Top:  $0 < t < 0.001$  s. Bottom:  $0.001 < t < 0.0015$  s.

steel is elastic the peaks in the strain profile are clear. For the standard crack model as well as for the  $G_f$ -type crack model the dependence of the crack spacing on the spatial discretisation (mesh size) and the time integration scheme (Newmark - average acceleration versus Newmark - damped) have been studied and the results are given in Figure 7. The same problems are observed as shown earlier for the case in which the slip contribution between concrete and reinforcement was left out of consideration. A primary crack occurs in one vertical row of finite elements and the spacing between the cracks is

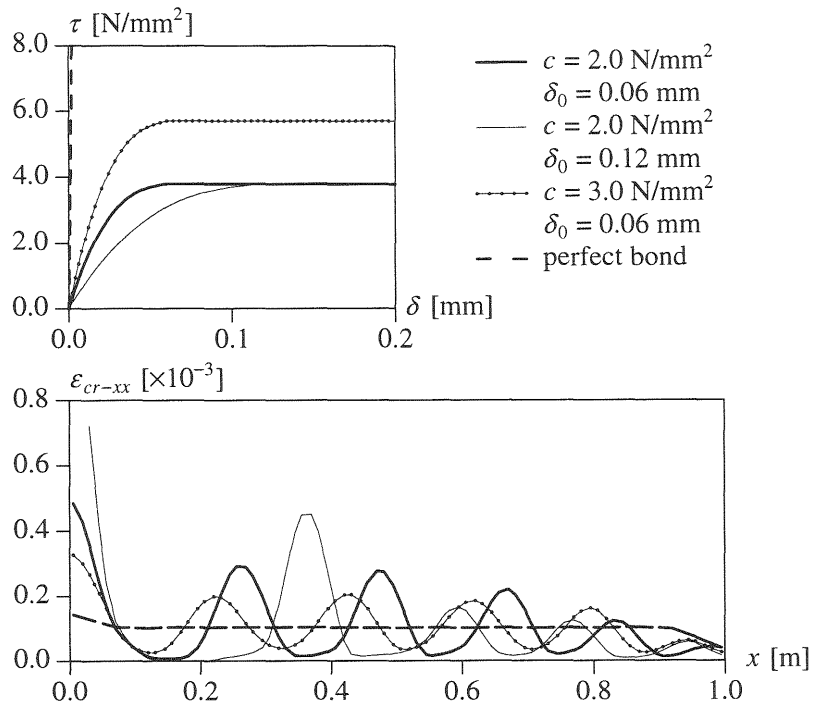


Fig. 11. Gradient crack model with  $l = 20$  mm - Mesh 2. Influence of the bond-slip characteristic.

influenced by the finite element size and the time integration procedure. The mesh dependence with respect to the crack spacing cannot be repaired by using a  $G_f$ -type crack model and for this reason global mesh objectivity for the strain energy consumption as obtained in plain concrete analyses with this model is not achieved.

For the gradient model with a length scale  $l = 20$  mm the non-objectivity in crack width and crack spacing is removed completely. The two meshes give the same results for the response in the concrete, the interface and the steel. The distance between the cracks is more or less constant  $l_s = 14.2$  mm. The influence of the length scale parameter  $l$  on the crack spacing  $l_s$  has been analysed in Figure 9. It is clear that the crack spacing is proportional to the length scale. A remarkable result is obtained for smaller length scales (see Figure 10). First, a pattern with cracks at regular distances occurs. Upon further loading it is observed that the crack spacing is reduced by a factor two and that the localised deformation of one out of two primary cracks continues.

Finally, the influence of the bond-slip characteristic on the crack spacing has been investigated. Three shear traction-slip curves have been considered. Next to the reference curve, both the level of deformation as the level of shear traction at which perfect slip occurs have been increased by a factor 2 and 1.5, respectively (see Figure 11). The curves show the crucial role that the bond-slip behaviour plays in the analysis. A stiffer bond-slip characteristic decreases the distance between the primary cracks while a softer bond-slip relation increases the value for the crack spacing. Again, perfect bond be-

tween concrete and reinforcement completely smooths out the inelastic deformations and a crack spacing cannot be observed.

## 5 Conclusions

The width and the spacing of primary cracks in reinforced elements have been studied. Attention is focused on the influence of the crack concept on the crack spacing. A comparison has been made between standard crack models and the gradient crack model. A fracture energy-type model prevents that the energy release per primary crack goes to zero upon mesh refinement but results for the crack spacing are completely arbitrary. Only the gradient model provides satisfactory results through the introduction of a length scale parameter. Mesh sensitivity with respect to the crack width and the crack spacing can be removed. The additional gradient parameter in the model can be coupled to the crack spacing measured in experiments. Furthermore, the crucial role of the bond-slip characteristic in predicting crack spacing in reinforced elements is determined.

## 6 Acknowledgements

Financial support of the Royal Netherlands Academy of Arts and Sciences to the first author is gratefully acknowledged.

## References

- Aifantis, E.C. (1984) On the microstructural origin of certain inelastic models. **J. Engng. Mater. Technol.**, 106, 326-334.
- Bazant, Z.P. and Oh, B. (1983) Crack band theory for fracture of concrete. **Mat. and Struct.**, 16, 155-177.
- Borst, R. de and Mühlhaus, H.-B. (1992) Gradient-dependent plasticity: Formulation and algorithmic aspects. **Int. J. Num. Meth. Eng.**, 35, 521-539.
- Dörr, K. (1980) Ein Beitrag zur Berechnung von Stahlbetonscheiben unter besonderer Berücksichtigung des Verbundverhaltens. Dissertation, Universität Darmstadt, Darmstadt.
- Lasry, D. and Belytschko, T. (1988) Localization limiters in transient problems. **Int. J. Solids and Struct.**, 24, 581-597.
- Mühlhaus, H.-B. and Aifantis, E.C. (1991) A variational principle for gradient plasticity. **Int. J. Solids and Struct.**, 28, 845-858.
- Pamin J. (1994) Gradient-dependent plasticity in numerical simulation of localization phenomena. Dissertation, Delft University of Technology, Delft.
- Pietruszczak, S. and Mroz, Z. (1981) Finite element analysis of deformation of strain softening materials. **Int. J. Num. Meth. Eng.**, 17, 327-334.
- Rots, J.G. (1988) Computational modeling of concrete fracture. Dissertation, Delft University of Technology, Delft.
- Sluys, L.J. (1992) Wave propagation, localisation and dispersion in softening solids. Dissertation, Delft University of Technology, Delft.

- 
- Sluys, L.J, Cauvern, M. and Borst, R. de. (1995) Discretization influence in strain-softening problems. **Eng. Comput.**, 12, 209-228.
- Willam, K. (1984) Experimental and computational aspects of concrete fracture, in **Proceedings International Conference on Computer Aided Analysis and Design of Concrete Structures** (eds. F. Damjanić et al.), Pineridge Press, Swansea, 33-70.

